MRS Advances (2022) 7:399–403
https://doi.org/10.1557/s43580-022-00260-z

ORIGINAL PAPER

Synergistic direct air capture of CO_2 with aqueous guanidine/amino acid solvents

Diāna Stamberga[1] · Nikki A. Thiele[1] · Radu Custelcean[1]

Received: 9 November 2021 / Accepted: 1 March 2022 / Published online: 8 March 2022

Abstract

Methylglyoxal-bis(iminoguanidine) (MGBIG) has been recently identified as a promising sorbent for direct air capture (DAC) of carbon dioxide via crystallization of guanidinium carbonate salts. In this study, the effects of aqueous amino acids and oligopeptides, such as glycine, sarcosine, serine, arginine, taurine, lysine, and glycylglycine, on the efficacy of DAC by crystallization of MGBIG carbonate have been investigated. While most of the amino acids studied were found to precipitate with MGBIG, thereby rendering the sorbent unavailable for DAC, sarcosine, the only amino acid in the series with a secondary amine group, remained soluble in the presence of MGBIG, leading to enhanced DAC compared to MGBIG alone. Specifically, for the same amount of MGBIG (5 mmol), the addition of a small amount of sarcosine to the aqueous solvent–as little as 0.5 mmol–led to extraction of six times as much CO_2 from the air (4.15 mmol vs. 0.7 mmol). Thus, aqueous MGBIG and sarcosine work in synergy, offering the prospect for an effective DAC process.

Introduction

Direct air capture (DAC) methods that separate carbon dioxide (CO_2) out of the atmosphere using engineered chemical processes offer the prospect of removing current CO_2 emissions from dispersed sources, and legacy CO_2 emissions, thereby keeping the atmospheric CO_2 concentration within safe limits with respect to climate change [1]. DAC processes are generally based on either solid sorbents [2] or aqueous solvents [3]. Recently, we introduced a new, phase-changing approach to DAC comprising CO_2 absorption by aqueous amino acids or peptides (as potassium salts) with the formation of (bi)carbonate anions, followed by carbonate crystallization with bis(iminoguanidines) (BIGs), as illustrated in Fig. 1 [4–6]. Mild heating of the BIG carbonate crystals at 60–120 °C releases the CO_2 and regenerates the BIG solid, thereby closing the CO_2 separation cycle. Ideally, this DAC approach combines the benefits of aqueous solvents and solid sorbents, such as easy scale up, low regeneration energies, and extended sorbent lifetime [7].

Thermodynamically, the DAC processes with amino acids and BIGs are driven to a large extent by the solubility difference between the initial BIG solid and the final BIG carbonate crystals. While most BIGs employed to date have low aqueous solubilities, in the range of 0.01 to 0.05 mol/L, the corresponding carbonate salts tend to be significantly less soluble, with solubility products in the same range as that of $CaCO_3$. The low solubilities of BIG carbonate salts can be attributed to a number of structural factors, such as strong hydrogen bonding between the carbonate anions and the guanidinium cations, the inclusion of water molecules in the crystals, which further stabilize the carbonate anions through hydrogen bonding, and π-stacking of the BIG cations [8]. All these interactions may, in principle, be designed and controlled through crystal engineering to optimize the DAC efficiency [9]. One key DAC performance that remains persistently suboptimal with BIGs is the relatively slow rate of CO_2 absorption due to limited aqueous solubilities and alkalinities of these guanidine compounds. Nonetheless, inclusion of aqueous amino acids or peptides in the DAC process significantly speeds up the otherwise slow CO_2 absorption by the aqueous BIG solutions [4–6]. The ready availability of relatively inexpensive amino acids or small oligopeptides, combined with the straightforward and modular synthesis of BIGs by imine condensation, offer a vast chemical matrix for designing DAC systems by simple mixing and matching to optimize key parameters such as cyclic CO_2 capacity, absorption rate, and sorbent regeneration energy.

✉ Radu Custelcean
custelceanr@ornl.gov

[1] Chemical Sciences Division, Oak Ridge National Laboratory, Oak Ridge, TN 37831, USA

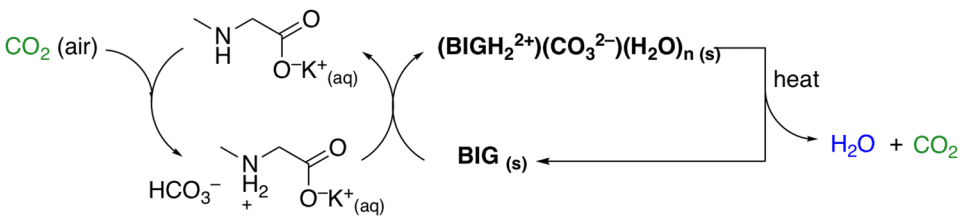

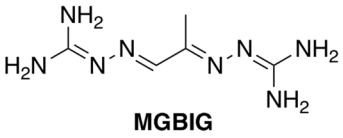

Fig. 1 DAC cycle via CO_2 absorption with aqueous amino acid salts (potassium sarcosinate is shown) and carbonate crystallization with BIGs. The chemical structure of MGBIG employed in this study is shown on the bottom

One particularly promising BIG recently developed in our labs is methylglyoxal-bis(iminoguanidine) (MGBIG). Its aqueous solubility of about 1 mol/L is significantly higher compared to analogous BIGs, which can be attributed to its increased molecular flexibility and the absence of π-stacking in the crystal structure [10]. As a result, MGBIG could in principle be employed as an aqueous solvent in a DAC process, an option not available with the less soluble BIG analogs. In the presence of atmospheric CO_2, MGBIG forms two main crystalline carbonate structures depending on the initial concentration of MGBIG. At concentrations greater than 0.75 M, MGBIG crystallizes primarily as $(MGBIGH^+)_2(CO_3^{2-})(H_2O)_2$, or phase 1 (P1). At concentrations lower than 0.3 M, MGBIG crystallizes mostly as $(MGBIGH_2^{2+})(CO_3^{2-})(H_2O)_2$, or phase 3 (P3). The crystal structures of these two MGBIG carbonate phases [10] are depicted in Fig. 2. The main difference between the two phases is the degree of MGBIG protonation: monoprotonated in P1, and di-protonated in P3. An important structural difference between the two phases is that in P1 the carbonate anion is only hydrogen-bonded by the guanidine groups (Fig. 2b), whereas in P3 it is hydrogen-bonded by guanidines and water molecules (Fig. 2e). Moreover, carbonate anions and water molecules form extended one-dimensional hydrogen-bonded chains in P3 (Fig. 2f). On the other hand, water molecules in P1 are isolated from the

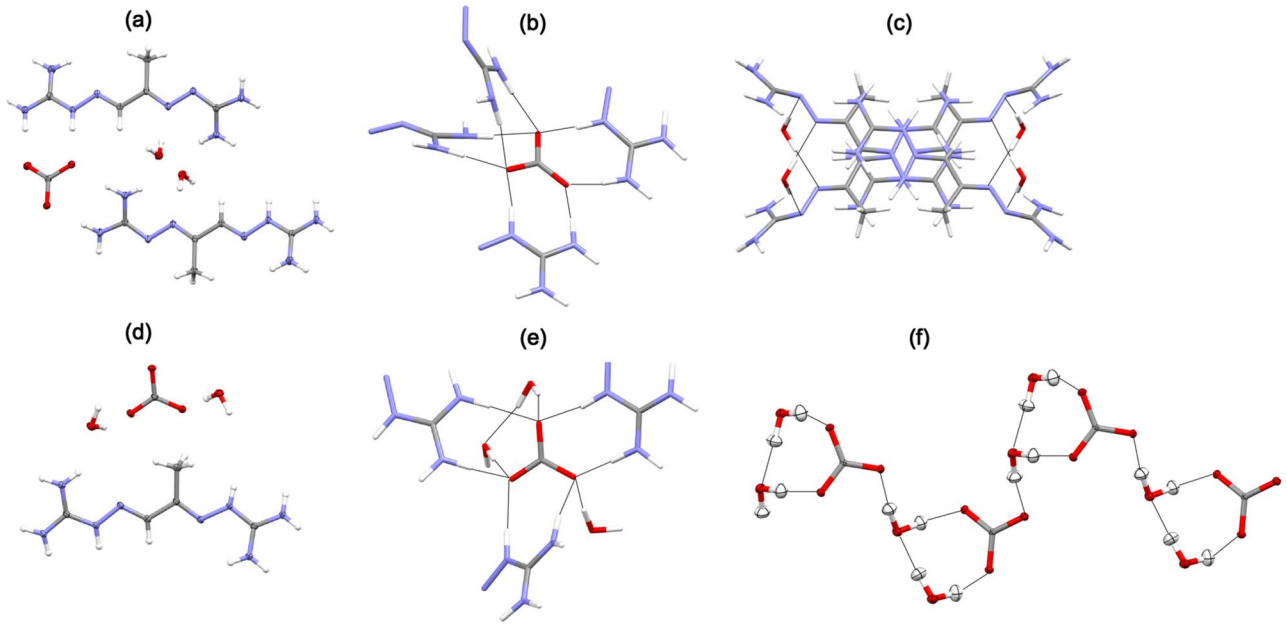

Fig. 2 Crystal structures of MGBIG carbonate P1 (**a**–**c**) and P3 (**d**–**f**), as determined by X-ray and neutron diffraction [10]. **a** ORTEP representation of P1. **b** Carbonate binding site in P1 consisting of 8 hydrogen bonds from the guanidine groups. **c** Water hydrogen bonding to guanidines in P1. **d** ORTEP representation of P3. **e** Carbonate binding site in P3 consisting of 6 hydrogen bonds from the guanidine groups and 3 hydrogen bonds from water molecules. **f** Extended hydrogen-bonded carbonate-water chains in P3

Scheme 1 Elementary steps involved in DAC with MGBIG

$$MGBIG_{(s)} \rightleftharpoons MGBIG_{(aq)} \quad (1)$$

$$MGBIG_{(aq)} + 2\,H_2O \rightleftharpoons MGBIGH_2^{2+}{}_{(aq)} + 2\,HO^-_{(aq)} \quad (2)$$

$$CO_{2(g)} \rightleftharpoons CO_{2(aq)} \quad (3)$$

$$CO_{2(aq)} + HO^-_{(aq)} \longrightarrow HCO_3^-{}_{(aq)} \quad (4)$$

$$HCO_3^-{}_{(aq)} + HO^-_{(aq)} \rightleftharpoons CO_3^{2-}{}_{(aq)} + H_2O \quad (5)$$

$$MGBIGH_2^{2+}{}_{(aq)} + CO_3^{2-}{}_{(aq)} + 2\,H_2O \rightleftharpoons MGBIGH_2(CO_3)(H_2O)_{2(s)} \quad (6)$$

$$MGBIG_{(s)} + CO_{2(g)} + 3\,H_2O \longrightarrow MGBIGH_2(CO_3)(H_2O)_{2(s)} \quad (7)$$

carbonate anions and are hydrogen-bonded to the guanidines instead (Fig. 2c). A metastable crystalline form, phase 2, comprising a mixture of mono- and di-protonated MGBIG, may also form at intermediate concentrations, though this form is rarely observed and therefore is not that relevant for a DAC process [10].

In this paper we report our preliminary results on the effects of amino acids on the DAC efficiency with aqueous MGBIG. This report includes the analysis of DAC with MGBIG alone, and combined with simple amino acids like glycine, sarcosine, serine, arginine, taurine, lysine, or with simple oligopeptides like glycylglycine. Based on this analysis, the most promising aqueous MGBIG/amino acid system was selected and further optimized to maximize the efficiency of the DAC process.

Materials and methods

Common reagents, including glycine, sarcosine, serine, arginine, taurine, lysine, glycylglycine, methylglyoxal, and aminoguanidine hydrochloride, were purchased from commercial suppliers and used without further purification. MGBIG was synthesized by a modified published procedure [10]. All water used was deionized (≥ 18 MΩ/cm). NMR spectra were collected using a Bruker Avance III 400 MHz NMR Spectrometer. Solubility measurements of MGBIG and $MGBIGH_2(CO_3)(H_2O)_2$, were done by UV–Vis spectroscopy, as previously described [10–12]. The acidity constants (pK_a) of MGBIG were determined by potentiometric titrations. The phase identities of the MGBIG-CO_3 crystals [10] from the DAC experiments were confirmed by single-crystal X-ray diffraction using a Bruker Quest D8 diffractometer with a Mo source ($\lambda = 0.71073$ Å). The two phases were identified based on their unit cell parameters measured at 100 K. P1: $a = 10.0437$, $b = 10.0656$, $c = 10.9849$, $\alpha = 90$, $\beta = 97.2500$, $\gamma = 90$; P3: $a = 7.0115$, $b = 8.6934$, $c = 21.6031$, $\alpha = 90$, $\beta = 96.3830$, $\gamma = 90$. Further experimental details and procedures are included in the Supplementary Information.

Results and discussion

Thermodynamic analysis of DAC with MGBIG

The elementary steps involved in DAC with MGBIG are illustrated in Scheme 1: dissolution of MGBIG in water (Eq. 1), MGBIG protonation by water to generate $MHBIGH_2^{2+}$ cations and HO^- anions (Eq. 2), CO_2 dissolution in water (Eq. 3), CO_2 reaction with HO^- to generate bicarbonate anions, HCO_3^- (Eq. 4), bicarbonate deprotonation by HO^- with formation of carbonate anions, CO_3^{2-} (Eq. 5), and crystallization of $MGBIGH_2(CO_3)(H_2O)_2$ (Eq. 6). The overall DAC reaction with MGBIG, leading to crystallization of $MGBIGH_2(CO_3)(H_2O)_2$, is represented by Eq. 7. For simplicity, only phase 3 of MGBIG-CO_3 is considered here, which is the only phase observed at low concentrations of MGBIG (< 0.3 mol/L).

The corresponding equilibrium constants for reactions 1–7 are listed in Table 1. The K values for reactions 1 and 6 were determined based on the measured solubility products of MGBIG and $MGBIGH_2(CO_3)(H_2O)_2$. The K value for reaction 2, representing the protonation of MGBIG in water ($K_{b1} \times K_{b2}$) was determined based on the acidity constants measured by potentiometric titrations. The K values for Reactions 3–5 are available in the literature [13–15].

The overall DAC reaction is highly favorable ($\log K = 5$), with a corresponding ΔG^o of –28.6 kJ/mol. The experimental standard free energy for the DAC process with MGBIG is in good agreement with the DFT-calculated value of – 30.6 kJ/mol reported previously [10].

Table 1 Equilibrium constants for the reactions involved in DAC with MGBIG

Equation	Reaction	K^a	Reference
1	MGBIG dissolution	1.1 M[b]	This study
2	MGBIG protonation	$10^{-11.51}$ M[2c]	This study
3	CO_2 dissolution	3.4×10^{-2} M atm^{-1}[d]	[13]
4	HCO_3^- formation	3×10^7 M^{-1}	[14]
5	CO_3^{2-} formation	4.68×10^3 M^{-1}[e]	[15]
6	$MGBIGH_2(CO_3)(H_2O)_2$ cryst	6.14×10^6 M^{-2}[f]	This study
7	Overall DAC reaction	1.00×10^5 atm^{-1}[g]	This study

[a]Determined at 25 °C

[b]$K_1 = K_{sp}$(MGBIG)

[c]$K_2 = (K_w)^2/(K_{a1}\times K_{a2})$; $K_{a1} = 10^{-7.55}$, $K_{a2} = 10^{-8.94}$

[d]$K_3 = K_H$ (Henry's solubility constant for CO_2)

[e]$K_5 = K_a(HCO_3^-)/K_w$

[f]$K_6 = 1/K_{sp}$(MGBIG-CO_3)

[g]$K_7 = K_1\times K_2\times K_3\times K_4\times K_5\times K_6$

DAC with aqueous MGBIG/amino acid solvents

Having determined that DAC with MGBIG is thermodynamically favorable, next we investigated the effect of combining MGBIG with amino acids on the efficiency of CO_2 absorption from air. Amino acids and small peptides have been found to significantly speed up atmospheric CO_2 capture processes with other BIGs [4–6]. In the previous systems, the DAC process comprised CO_2 absorption with aqueous amino acid salts (amino acid + KOH) in a first step, followed by (bi)carbonate crystallization with solid BIGs in a subsequent step. In the current system, the high aqueous solubility of MGBIG allows for the two reactions to be combined into one pot. Another potential advantage of combining amino acids and MGBIG solutions is that the guanidine groups can act as bases that deprotonate and activate the amino groups for reaction with CO_2, thereby circumventing the need to use KOH base.

DAC with aqueous amino acid/MGBIG solutions was tested with the glycine (Gly), serine (Ser), sarcosine (Sar), taurine (Tau), arginine (Arg), and lysine (Lys) amino acids, as well as with the glycylglycine (GlyGly) peptide. In the initial screening experiments, 10 mL solutions containing 0.5 M MGBIG and 0.5 M amino acid were placed in 20 mL vials and left open to air for 1 week. Formation of solid precipitates was observed in each vial, and the reactions were quantified with ^{1}H NMR spectroscopy using dimethylsulfone as an internal standard to determine the amounts of MGBIG and amino acids precipitated. As documented in Table 2, except for Sar, every amino acid precipitated from solution in significant amount, along with MGBIG, suggesting chemical reactions between MGBIG and the amino acids occurred. Such reactions

Table 2 Screening of DAC with aqueous MGBIG (0.48 ± 0.06 M) and amino acids (0.50 ± 0.08 M) for 1 week

Amino acid/peptide	$[AA]_i$	$[AA]_f$	$[MGBIG]_i$	$[MGBIG]_f$
Gly	0.47	0.28	0.44	0.25
GlyGly	0.55	0.41	0.53	0.45
Ser	0.52	0.38	0.48	0.29
Sar	**0.49**	**0.46**	**0.47**	**0.26**
Tau	0.54	0.43	0.48	0.38
Arg	0.51	0.26	0.48	0.26
Lys	0.44	0.23	0.46	0.27

The initial and final concentrations (M) were determined by quantitative NMR using dimethylsulfone as an internal standard. Sar (bold) was selected for further studies based on its negligible precipitation

are not desirable in a DAC process, in which ideally the amino acid facilitates the CO_2 capture while remaining in solution, whereas MGBIG crystallizes as a carbonate salt (Fig. 1). On the other hand, a negligible amount of Sar was found to be removed from solution by precipitation, prompting us to select this amino acid for further studies.

In the next set of DAC experiments, we investigated the effect of Sar concentration on the MGBIG carbonate crystallization yield and the crystalline phase formed. Keeping the initial concentration of MGBIG to 0.5 M, the concentration of Sar was varied from 0 to 0.5 M. The observed yields of crystallization, measured as the mol% of MGBIG removed from solution after 2 weeks of exposure to open air, are plotted in Fig. 3. The phase identities of the crystallized solids were determined by optical microscopy and X-ray diffraction. P1 and P3 of MGBIG-CO_3 have very different morphologies, prisms and needles, respectively, making the differentiation straightforward by optical microscopy. These phases were additionally confirmed by single-crystal X-ray diffraction. As illustrated in Fig. 3, in the absence of Sar, P1 MGBIG-CO_3 crystallized in 28% yield. On the other hand, only 0.05 M Sar was sufficient to induce a switch to P3 MGBIG-CO_3, and a significant boost in the crystallization yield to 83%. The yield of MGBIG-CO_3 P3 crystallization remained virtually constant up to 0.3 M MGBIG, and then it slightly declined at 0.4 and 0.5 M MGBIG concentrations. Thus, addition of Sar caused a dramatic improvement in DAC by crystallization of MGBIG-CO_3. We note here that crystallization of P3 is preferred over P1, as the former requires only one equivalent of MGBIG vs two equivalents for the latter, for each equivalent of carbonate removed from solution. For the same amount of MGBIG (5 mmol), addition of a small amount of Sar–as little as 0.5 mmol–results in six times as much CO_2 extracted from the air (4.15 mmol vs. 0.7 mmol). Thus, MGBIG and Sar work in synergy, leading to enhanced DAC. Scale-up efforts and the design and development of a DAC process based on the aqueous MGBIG/Sar solvent are currently under way.

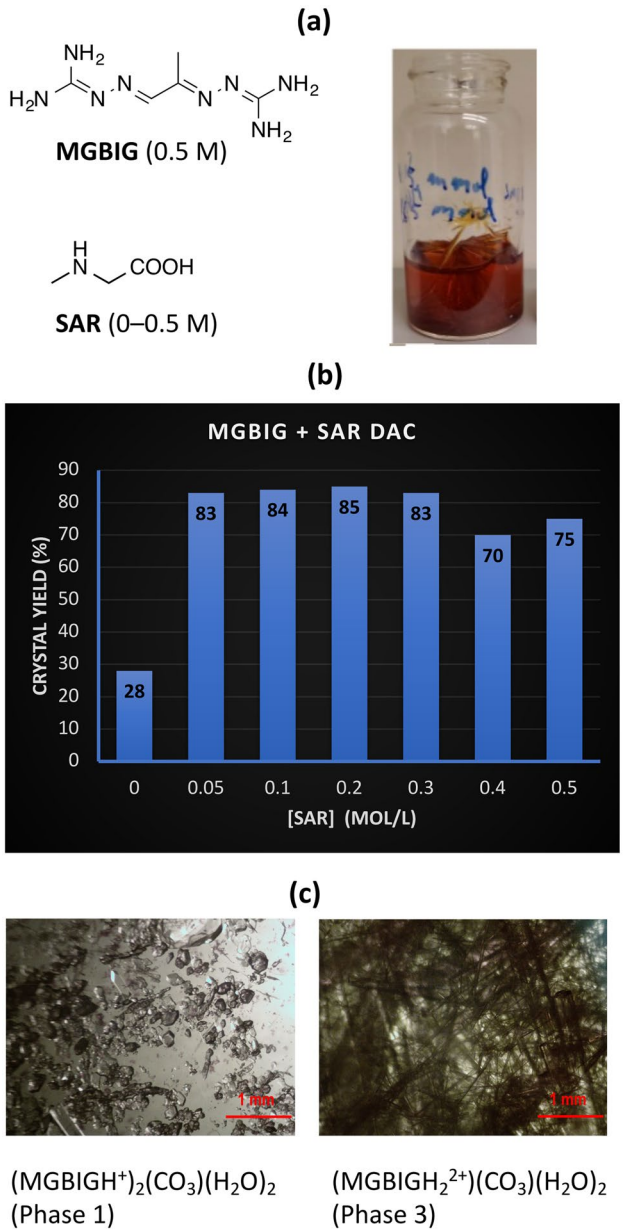

Fig. 3 DAC with aqueous MGBIG/SAR. **a** Typical crystallization experiment, with 0.5 M MGBIG and variable initial concentrations of SAR (0–0.5 M). **b** Measured MGBIG-CO_3 crystallization yields after 2 weeks, as a function of SAR concentration. **c** Optical micrographs of phase 1 and phase 3 MGBIG-CO_3 formed in the absence and presence of SAR, respectively

Conclusions

The effects of amino acids and small oligopeptides, such as glycine, sarcosine, serine, arginine, taurine, lysine, and glycylglycine, on the efficacy of DAC by crystallization of MGBIG carbonate from aqueous solutions, have been investigated. Sarcosine, a secondary amino acid, dramatically improves DAC by crystallization of MGBIG-CO_3, while the other amino acids precipitate with MGBIG, rendering it unavailable for DAC. In the case of sarcosine, addition of a small amount of this amino acid–as little as 0.5 mmol–to a 0.5 M aqueous solution of MGBIG, led to a six-fold increase in the amount of CO_2 extracted from the air (4.15 mmol vs. 0.7 mmol). Thus, aqueous MGBIG and sarcosine work in synergy, offering the prospect for an effective DAC process.

Supplementary Information The online version contains supplementary material available at https://doi.org/10.1557/s43580-022-00260-z.

Acknowledgments This work was supported by the US Department of Energy, Office of Science, Basic Energy Sciences, Chemical Sciences, Geosciences, and Biosciences Division. The manuscript was produced by UT-Battelle, LLC under Contract No. DE-AC05-00OR22725 with the U.S. Department of Energy. The publisher acknowledges the U.S. Government license to provide public access under the DOE Public Access Plan (http://energy.gov/downloads/doe-public-access-plan).

Data availability The data that support the findings of this study are available from the corresponding author upon request.

Declarations

Conflict of interest R.C. is an inventor on a patent on DAC involving aqueous amino acid solvents and crystalline guanidines, and seeks to commercialize a technology based on the approach presented in this manuscript.

References

1. N. McQueen, K.V. Gomes, C. McCormick, K. Blumanthal, M. Pisciotta, J. Wilcox, Prog. Energy **3**, 032001 (2021)
2. X. Shi, H. Xiao, H. Azarabadi, J. Song, X. Wu, X. Chen, K.S. Lackner, Angew. Chem. Int. Ed. **59**, 6984–7006 (2020)
3. E.S. Sanz-Perez, C.R. Murdock, S.A. Didas, C.W. Jones, Chem. Rev. **116**, 11840–11876 (2016)
4. F.M. Brethomé, N.J. Williams, C.A. Seipp, M.K. Kidder, R. Custelcean, Nat. Energy **3**, 553–559 (2018)
5. R. Custelcean, N.J. Williams, K.A. Garrabrant, P. Agullo, F.M. Brethomé, H.J. Martin, M.K. Kidder, Ind. Eng. Chem. Res. **58**, 23338–23346 (2019)
6. R. Custelcean, K.A. Garrabrant, P. Agullo, N.J. Williams, Cell Rep. Phys. Sci. **2**, 100385 (2021)
7. R. Custelcean, Chem **7**, 2848–2852 (2021)
8. C.G. Gianopoulos, Z. Chua, V.V. Zhurov, C.A. Seipp, X. Wang, R. Custelcean, A.A. Pinkerton, IUCrJ **6**, 56–65 (2019)
9. R. Custelcean, Chem. Sci. **12**, 12518–12528 (2021)
10. R. Custelcean, N.J. Williams, X. Wang, K.A. Garrabrant, H.J. Martin, M.K. Kidder, A.S. Ivanov, V.S. Bryantsev, Chemsuschem **13**, 6381–6390 (2020)
11. R. Custelcean, N.J. Williams, C.A. Seipp, A.S. Ivanov, V.S. Bryantsev, Chem. Eur. J. **22**, 1997 (2016)
12. N.J. Williams, C.A. Seipp, F.M. Brethomé, Y.-Z. Ma, A.S. Ivanov, V.S. Bryantsev, M.K. Kidder, H.J. Martin, E. Holguin, K.A. Garrabrant, R. Custelcean, Chem **5**, 719–730 (2019)
13. J.J. Carroll, J.D. Slupsky, A.E. Mather, J. Phys. Chem. Ref. Data **20**, 1201–1209 (1991)
14. X. Wang, W. Conway, R. Burns, N. McCann, M. Maeder, J. Phys. Chem. A **114**, 1734–1740 (2010)
15. S.K. Lower, *Carbonate Equilibria in Natural Waters* (Simon Fraser University, Burnaby, 1996)